Chapter 5.

Quantitative Analysis of Multivalent Interactions of Carbohydrate-Encapsulated Gold Nanoparticles with Viscum Album Agglutinin I

5.1. Introduction

Gold nanoparticles with biomolecules encapsulated on their surface have recently attracted great interests because of their various applications for biological labeling, analyzing and sensing.[1-4] Since more than a decade ago, many rapid diagnostic kits have been developed and used commercially based on the well-controlled interaction between antibody conjugated gold nanoparticles and their target antigens.[5] Besides the conjugates with antibody, bio-functionalized gold nanoparticles were also prepared by covalently binding DNA, carbohydrates or other bio-receptor ligands onto the nanoparticle surface. New biological applications based on those functionalized gold nanoparticles have being developed for the uses of DNA detection, gene expression, molecular recognition, bacteria[6] and tissue growth.[7] For examples, gold nanoparticles attached with single strain DNA have been applied for the colorimetric detection of targeted complimentary DNA sequence.[8-10] Carbohydrate encapsulated gold nanoparticles have been used as a probe to identify the specific protein of pili on a *E. Coli*.[3] Also, self-assembled poly-(ethylene-glycol)-derived carbohydrates were synthesized for the colorimetric

detection of recinus communis agglutinin.[4] In addition, new chemical probes to quantify the presence of unknown metal ions have been explored using gold nanoparticles encapsulated with the corresponding receptors.[11-14] Because of the unique structural (large surface area to volume ratio) and optical (surface plasmon absorption) properties of gold nanoparticles, new bio-functionalized gold nanoparticles and their potential applications have being explored in the fields of material, biological and medical researches.

Gold nanoparticles encapsulated with carbohydrates (*carbohydrate*-AuNP) are particularly important for the bio-medical applications because carbohydrates play vital roles in many biological processes including the interactions of bacteria, viruses and cancer with host cell, cell-cell recognitions, immune responses, and tissue growth and repairs.[15-18] In *carbohydrate*-AuNP system, gold nanoparticles serve as a ligand carrier and *carbohydrate*-AuNPs act as a bio-molecule. The *carbohydrate*-AuNPs are expected to generate stronger interactions or effects during a protein recognition process in comparison to the corresponding mono carbohydrate ligand. The strong multivalent interaction of the *carbohydrate*-AuNP to lectin was mainly attributed to a large number of carbohydrate molecules assembled on nanoparticle surface. The multivalent interaction between cell surface receptors and carbohydrates has been discovered in many biological systems.[19] A number of diverse carbohydrate carriers have been presented for multivalent interaction between the carbohydrates and lectin including low-molecular weight displays,[20] copolymers,[21] dendrimers,[22] liposomes[23] and nanoparticles.[24] For examples, the

artificial multivalent system, which was prepared by covalently binding multiple carbohydrates on a short chain polymer, has shown the great enhancement on the binding affinity and specificity to the lectin.[3] Recently, we have demonstrated that gold nanoparticle serves as a multivalent ligand carrier of carbohydrate. The enhancement of binding affinity of *carbohydrate*-AuNP to the concanavalin A (Con A) has been studied by the surface plasmon resonance (SPR) technique using a BIAcore system.[25] More importantly, we found that the enhancement of binding affinity was strongly correlated with the linker lengths of the carbohydrate and the sizes of gold nanoparticle. The results showed that the binding affinities of *carbohydrate*-AuNP to Con A were better than the corresponding mono-mannose.

In this chapter, we have extended our investigations of the multivalent interaction between *carbohydrate*-AuNP and lectins. A series of gold nanoparticles encapsulated with different types of carbohydrates were synthesized and characterized as listed in chapter 2 (Experience section). The multivalent interactions were studied by utilizing the SPR technique to quantitatively analyze the binding affinity between the *carbohydrate*-AuNP and lectin (Figure 5-1).

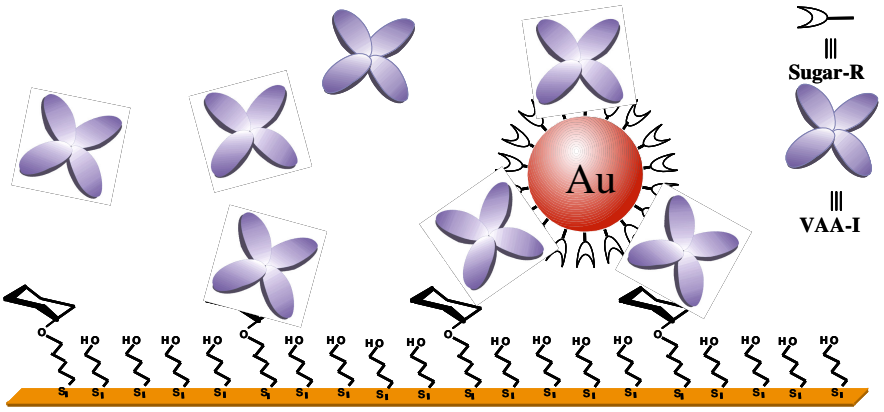

Figure 5-1. BIAcore measurement by J1 Chip of binding affinity between VAA-I and *carbohydrate*-AuNP.

The relative inhibition potency (RIP) was calculated among different *carbohydrate*-AuNP. The results showed that the binding galactose coated AuNP (*s*-6-*t*-AuNP, *s*- and *l*-20-*t*-AuNP) to Viscum album agglutinin I (VAA-I, also referred to as mistletoe lectin I, see Figure 5-2), exhibited a strong multivalent effect, and the binding specificity between *carbohydrate*-AuNP and the lectin was similar to that of the monovalent counterparts.

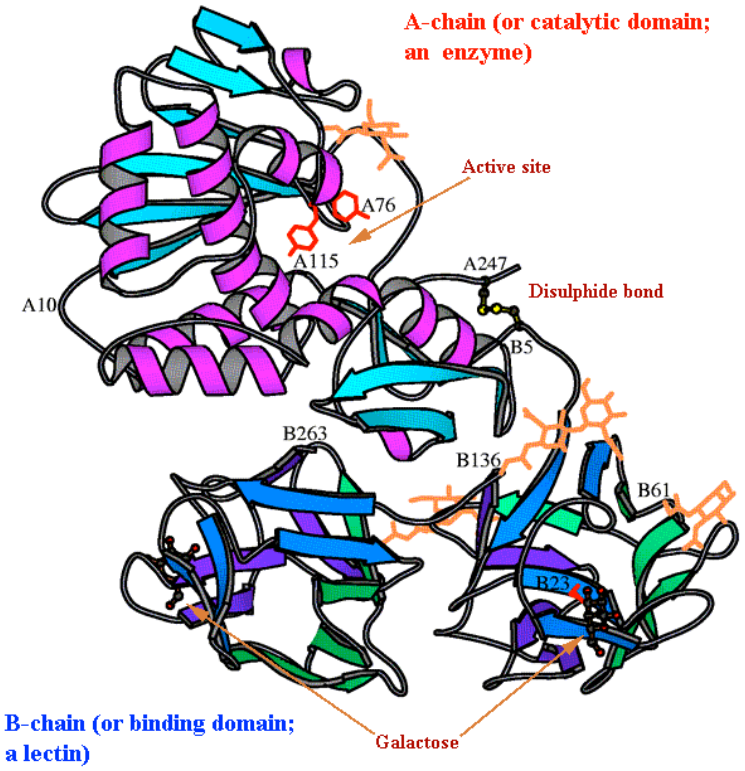

Figure 5-2. The protein structure of Con A.

Also, the divalent binding ability to VAA-I tetramer of galactose ligands encapsulated on AuNPs is relevantly greater in *s*- and *l*-20-*t*-AuNP than in *s*-6-*t*-AuNP and the binding affinity (ie. RIP) of *l*-20-*t*-AuNP is greater than *s*-20-*t*-AuNP. The length effects of galactopyranosides encapsulated on AuNP have also been observed in the binding experiments of *s*-6-*t*-AuNP, *s*- and *l*-20-*t*-AuNP to VAA-I. The relative inhibit potency values compared between *carbohydrate*-AuNPs indicates that the larger size of AuNP and the carbohydrate ligand with longer linker length showed excellent binding affinity in VAA-I. Our results demonstrate that gold nanoparticles can be excellent multivalent carbohydrate carriers. Our studies in

this section gives more confident result to open a new route for designing new inhibitors and biological effectors in a biological system based on *carbohydrate*-AuNP.

5.2. Results

The lectin and *carbohydrate*-AuNP, for examples *l*-20-*t*-AuNP with VAA-I, respectively, mixture (50 μL) was injected to mannose coated J1 chip and the flow rate was controlled at a 60 μL/minute. The equilibrium binding response values was collected at equilibrium binding portion of the curve (300 seconds post-injection). A set of SPR response curves was obtained after different concentrations of the inhibitor solution were applied. K_i value were determined by fitting the data into the equation: $f = [I]/([I] + K_i\ (1 + F/K_d)$.[26,27] In competition binding assays of VAA-I, for examples we measured the binding responses of 0.5 μM VAA-I tetramer with different concentrations of βMeGal, *s*-6-*t*-AuNP, or *l*-20-*t*-AuNP as competitive inhibitors to generate inhibition curves, see Figure 5-3, 5-4 and 5-5.

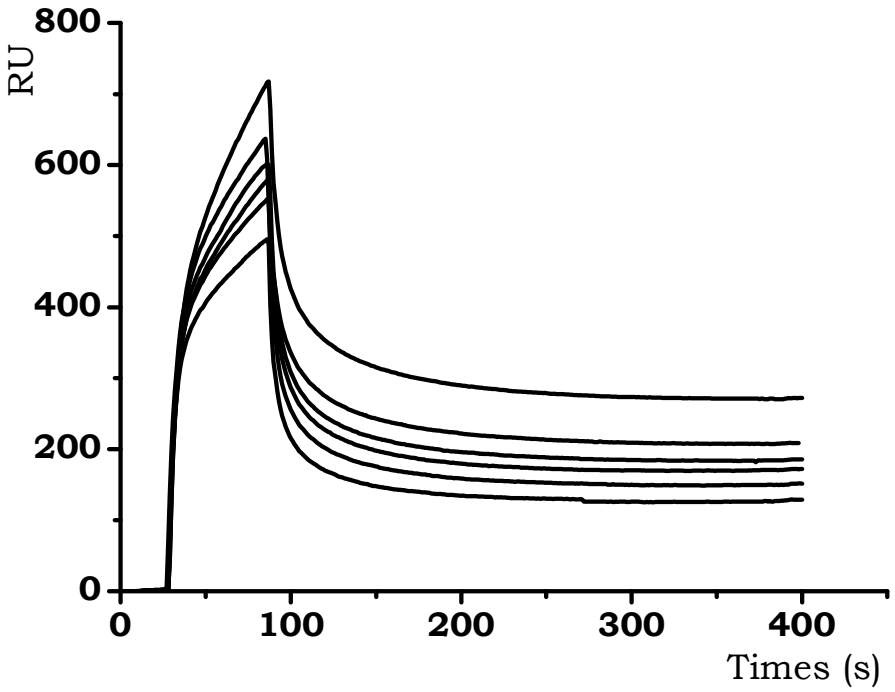

Figure 5-3. A set of curves for 0, 0.75, 1.5, 3, 6, 12 μM βMeGal of VAA-I (top to bottom) were showed.

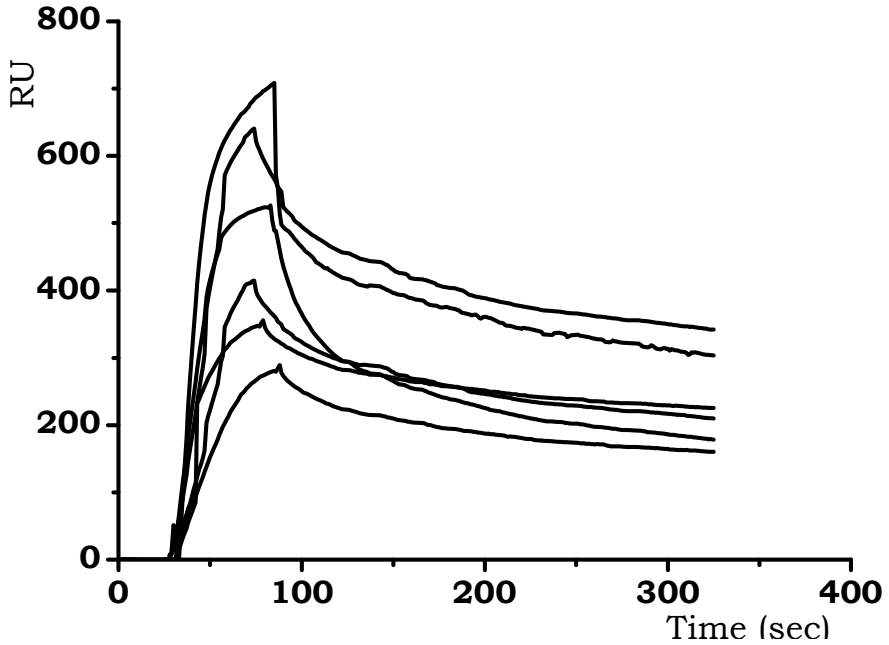

Figure 5-4. A set of curves for 0, 0.01, 0.02, 0.05, 0.11, 0.22 μM *s*-6-*t*-AuNP of VAA-I (top to bottom) were showed.

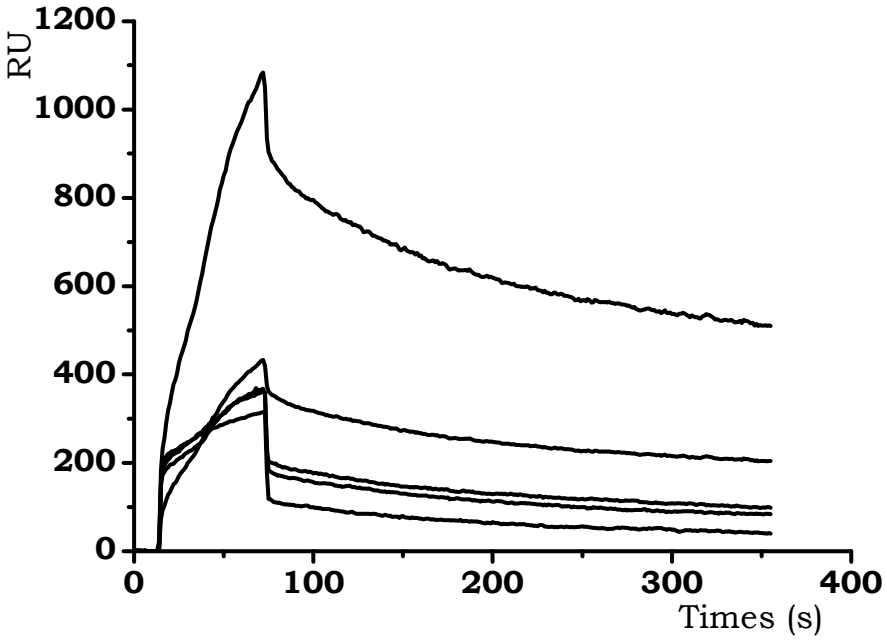

Figure 5-5. A set of curves for 0, 0.003, 0.012, 0.06, 0.12 μM *l*-20-*t*-AuNP of VAA-I (top to bottom) were showed.

From the inhibition curves of serious galactopyranoside encapsulated gold nanoparticles, the inhibition constant (K_i) was obtained using the equations derived by Attie *et al.*.[28] To compare the inhibition potencies of the individual galactose ligand on *s*-6-*t*-AuNP, *s*- and *l*-20-*t*-AuNP to monovalent βMeGal, we generated by measuring the binding responses for 0.5 μM VAA-I tetramer with βMeGal and *l*-20-*t*-AuNP, and the RIPs and K_is of *s*-6-*t*-AuNP, *s*- and *l*-20-*t*-AuNP, as listed in Table 5.[29]

Compound	K_i	RIP
βMeGal	1.8×10^{-5}	1.0
6-*t*-AuNP	6.8×10^{-9}	14.7
s-20-*t*-AuNP	2.2×10^{-10}	138.6
l-20-*t*-AuNP	4.3×10^{-10}	55.1
6-*m*-AuNP	2.7×10^{-8}	／
6-*g*-AuNP	—	—

— : no inhibition; ／ :not determined

Table 5. The data of dissociation constants (Ki) and relative inhibition potency (RIP) of *carbohydrate*-AuNP to VAA-I.

The RIP values of *s*-6-*t*-AuNP, *s*- and *l*-20-*t*-AuNP are ranged from 14 to 138 (Table 5), indicating that the galactose ligands on *carbohydrate*-AuNPs enhanced affinities by one to two orders to VAA-I than those of galactose monomer, respectively. In addition, *s*-6-*t*-AuNP, *s*- and *l*-20-*t*-AuNP exhibited a stronger inhibition effect than those of *s*-6-*g*-AuNP and *s*-6-*m*-AuNP. Moreover, *s*-6-*g*-AuNP and *s*-6-*m*-AuNP displayed no noticeable changes in inhibition effect. These observations are consistent with the previous studies that VAA-I binds to galactose better than mannose but does not bind to glucose.[30,31] It has been known that the binding affinity of VAA-I with galactose is higher than that with mannose.[30] Similar binding affinity tendency was also observed when the *carbohydrate*-AuNPs were used.

5.3. Discussion

The detailed structures of the lectins are expected to strongly correlate with the binding model between *carbohydrate*-AuNP and lectin. It has been reported that Con A exits as a tetramer complex under pH=7 and binds specifically to manno- and glucopyranosides.[32] In this tetrameric complex, there are two binding sites available on the same surface plane with the distance by 6.5 nm.[33] VAA-I is a heterodimeric two-chain (type II) ribosome-inactivating protein consisting of a catalytically active A-chain with rRNA N-glycosidase activity and a B-Chain with carbohydrate binding specificity.[34,35] VAA-I has been reported as a specific galactoside- or lactose-binding lectin in which two carbohydrate binding sites on each face of the complex are separated by 4.7 nm.[30] Although the configuration of Con A and VAA-I complexes are different, but the average size of *carbohydrate-* AuNP are comparable to the distance between two carbohydrate binding sites. To compare the inhibition potencies between each *carbohydrate*-AuNP with VAA-I, we provided a rationale for explaining the affinities obtained by SPR competition assays (see Tables 5). As the particle diameters of *s*-6-*t*-AuNP, *s*- and *l*-20-*t*-AuNP are comparable to and significantly larger than the distance between two relevant binding sites on VAA-I complex, respectively.

In order to compare the inhibition capability between all inhibitors more specifically, we calculate average relative inhibition capability of each inhibitor to VAA-I. The RIP values of *s*-6-*t*-AuNP, *s*- and *l*-20-*t*-AuNP are ranged from 14 to 138 (Table 5), indicating that the multivalent galactose ligands on AuNPs enhanced

affinities by one to two orders to VAA-I than those of monovalent galactose ligands, respectively. The RIP values of *s*-6-*t*-AuNP, *s*- and *l*-20-*t*-AuNP, shown in Table 5, indicate the binding potency of each galactose on AuNP is higher than free galactose, because free galactose can only interact with the lectin by a mono-binding mode but not multi-binding model presented by *s*-6-*t*-AuNP, *s*- and *l*-20-*t*-AuNP. Therefore, we conclude that the carbohydrate encapsulated AuNP can provide multivalence effect and its inhibition effect is always much greater than free carbohydrate.

In the size effect, when the nanoparticles become bigger, its surface area becomes larger. Thus, more carbohydrate ligands can be assembled on its surface resulting in increasing its binding affinity with target lectin. In the ligand length effect, compared the sizes of *l*-20-*t*-AuNP and *s*-20-*t*-AuNP with VAA-I complex, both particle diameters are significantly larger than the distance between two relevant binding sites on VAA-I complex. However, the binding affinity of *l*-20-*t*-AuNP is stronger than that of *s*-20-*t*-AuNP, this might be attributed to the differences in their intrinsic properties, for example, the orientation of galactose groups on the surface and/or the rigidity of the linkers. Although the number of carbohydrate on *l*-20-*t*-AuNP is more than that of *s*-20-*t*-AuNP, the effect of the RIP value is smaller. Because the distance of two binding sites of lectin complex is constant, it seems that each carbohydrate encapsulated on *s*-20-*t*-AuNP is arrayed more compactly while the carbohydrates on *l*-20-*t*-AuNP are too densely. Thus, many carbohydrates can not effectively bond onto binding site of lectin and the carbohydrates probably be wasted. The distance effect of carbohydrate displays in the results of RIP value that

long linker *l*-20-*t*-AuNP is nearly a half of the short linker *s*-20-*t*-AuNP.

Overall, we observed essentially no switch of VAA-I specificities for carbohydrates clustered on nanoparticles in our systems. Taken together, our results provide strong evidence that clustering of carbohydrate ligands on a nanoparticle significantly enhances the ligand binding affinities with lectins in a specific recognition. Also, we showed that *carbohydrate*-AuNP scaffolds are relatively easy to be assembled and the affinity of *carbohydrate*-AuNP to lectin can be adjusted by altering nanoparticle size or sugar moiety.

5.4. Conclusion

We have demonstrated that AuNP is a good multivalent ligand carrier. The multivalent interactions between *s*-6-*t*-AuNP, *s*- and *l*-20-*t*-AuNP with VAA-I are affected by nanoparticle size and the linker length of carbohydrate ligands. The affinity between *carbohydrate*-AuNP and target lectin can be easily enhanced by multivalent effect. Our approaches may be also applicable to other types of nanoparticles such as quantum dots[36] and magnetic nanoparticles.